OXFORD

Cerebral Cortex, July 2020;30: 3884–3894

doi: 10.1093/cercor/bhaa004
Advance Access Publication Date: 17 February 2020
Original Article

ORIGINAL ARTICLE

Prefrontal Cortical Reactivity and Connectivity Markers Distinguish Youth Depression from Healthy Youth

Prabhjot Dhami[1,2], Sravya Atluri[1,3], Jonathan C. Lee[1,2,4], Yuliya Knyahnytska[1,4], Paul E. Croarkin[5], Daniel M. Blumberger[1,2,4], Zafiris J. Daskalakis[1,2,4] and Faranak Farzan[1,2,4,6]

[1]Temerty Centre for Therapeutic Brain Intervention, Centre for Addiction and Mental Health, Toronto, Ontario M6J 1A8, Canada, [2]Institute of Medical Science, Faculty of Medicine, University of Toronto, Toronto, Ontario, M5S 1A8, Canada, [3]Institute of Biomaterial and Biomedical Engineering, University of Toronto, Toronto, Ontario M5S 3G9, Canada, [4]Department of Psychiatry, University of Toronto, Toronto, Ontario M5T 1R8, Canada, [5]Mayo Clinic Depression Center, Mayo Clinic, Rochester, MN, USA and [6]Centre for Engineering-led Brain Research (eBrain Lab), School of Mechatronic Systems Engineering, Surrey, British Columbia V3T 0A3, Canada

Address correspondence to Faranak Farzan, School of Mechatronic Systems Engineering, Simon Fraser University, 250-13450 102 Avenue, Surrey, British Columbia V3T 0A3, Canada. Email: ffarzan@sfu.ca

Abstract

Up to 50% of youth with depression do not respond to conventional first-line treatments. However, little research has been conducted on the pathophysiology of youth depression, hindering the identification of more effective treatments. Our goal was to identify neurophysiological markers that differentiate youth with depression from healthy youth and could serve as targets of novel treatments. We hypothesized that youth with depression would exhibit network-specific cortical reactivity and connectivity abnormalities compared with healthy youth. Transcranial magnetic stimulation combined with electroencephalography and magnetic resonance imaging was employed in combination with clinical and behavioral assessments to study cortical reactivity and connectivity in bilateral dorsolateral prefrontal cortex (DLPFC), motor cortex, and inferior parietal lobule, sites linked to the frontoparietal network, sensorimotor network, and default mode network, respectively. In youth depression, greater cortical reactivity was observed specific to the left and right DLPFC stimulation only, which correlated with anhedonia scores. Additionally, the connectivity of the right DLPFC was significantly higher in youth depression. Source reconstruction attributed the observed connectivity dysregulation to regions belonging to the default mode network. The neurophysiological signatures identified in this study have high potential to inform the development of more effective and targeted interventions for the youth depression population.

Key words: adolescence, depression, EEG, TMS, youth

Introduction

Major depressive disorder (MDD) in youth is a debilitating illness that exacts enormous social, economic, and personal cost. An estimated 30–50% of youth do not respond to conventional treatments (March et al. 2007). There are also ongoing controversies regarding the safety of standard antidepressants in individuals younger than 24 years of age (Gibbons et al. 2012). This suggests

© The Author(s) 2020. Published by Oxford University Press. All rights reserved. For permissions, please e-mail: journals.permissions@oup.com

that treatment alternatives with similar or greater efficacy and a more favorable safety profile are needed for this population. In order to achieve this, a greater understanding of the pathophysiology of youth MDD is needed to develop treatments that are optimally targeted at the underlying impairments.

MDD is associated with the dysregulation of cortical inhibitory and excitatory mechanisms, as well as large-scale functional networks. Transcranial magnetic stimulation (TMS) metrics of cortical inhibition and excitation, which involves the activation of larger neuronal populations, are known to be altered in the prefrontal cortex and motor cortex of depressed adults (Levinson et al. 2010; Voineskos et al. 2018). MDD is also associated with alterations in the functional connectivity of various brain networks, including the frontoparietal and default mode network (Kaiser et al. 2015).

Despite the growing evidence in support of neurophysiological alterations in depression, the vast majority of these studies have focused on adults. Youth is a period characterized by substantial structural and functional development (Gogtay et al. 2004; Giedd et al. 2008). It may be inaccurate to simply assume that findings from the adult MDD literature are translatable to youth MDD, as the underlying neurobiology of depression in both age groups may differ (Zalsman et al. 2006). Indeed, various markers of excitation, inhibition, and connectivity are known to be age dependent (Blakemore and Choudhury 2006; Fung et al. 2010; Croarkin et al. 2014). Furthermore, conventional youth MDD treatments, which only have modest efficacy (March et al. 2007), are developed and based on adult research. Thus, it is critical to specifically study the pathophysiology of youth MDD.

To address this gap in the literature, we used TMS paired with electroencephalography (TMS-EEG) to investigate the differences in cortical excitation, inhibition, and connectivity between youth MDD and healthy youth. Single pulse TMS-EEG elicits multiple TMS-evoked potentials (TEPs) which have been shown to reflect activation of distinct excitatory and inhibitory mechanisms (Premoli et al. 2014; Darmani and Ziemann 2019); such neurophysiological measures have yet to be assessed in the youth MDD population. TMS-EEG can also provide measures of causal connectivity, as the activation induced by TMS in a local and targeted area propagates to other anatomically and functionally connected regions (Bortoletto et al. 2015). Functional connectivity neuroimaging studies to date suggest youth MDD to be associated with functional connectivity alterations (Miller et al. 2015), but such analyses lack the description of electrophysiology-related frequency-specificity or directionality and causality between regions that can be provided by TMS-EEG.

Six distinct cortical regions of interest across both hemispheres were selected for assaying: bilateral dorsolateral prefrontal cortex (DLPFC), motor cortex, and inferior parietal lobules (IPL). As MDD is associated with large-scale network dysfunctions (Kaiser et al. 2015), we assayed these six cortical areas as they belong to discrete functional networks; the DLPFC is part of the frontoparietal network, the motor cortex is part of the sensorimotor network, and the IPL is a node of the default mode network (Damoiseaux et al. 2006; van den Heuvel and Hulshoff Pol 2010). By assaying the selected cortical sites, we aimed to determine whether alterations in neurophysiology, as measured by TMS-EEG, were potentially region and network specific.

As the pathophysiology of MDD has been linked to changes in prefrontal regions (Koenigs and Grafman 2009), along with the prefrontal cortex of those with depression being found to exhibit excessive cortical reactivity (Voineskos et al. 2018) and functional connectivity (Leuchter et al. 2012), we hypothesized that youth MDD would exhibit significantly greater cortical reactivity and connectivity measures following DLPFC stimulation only.

Materials and Methods

Patient Sample

Recruitment

Youth aged 16–24 years old were recruited from the community through print- and web-based posters, hospital research registries, physician referrals, and clinics at the Centre for Addiction and Mental Health in Toronto. All participants provided written informed consent and the protocols were approved by Centre for Addiction and Mental Health in accordance with the Declaration of Helsinki.

Eligibility

In total, 45 youth MDD and 20 healthy youth controls were recruited. Eligible patients were outpatients on stable treatment (medication or psychotherapy) for 4 weeks prior to testing; between the ages of 16 and 24; with a Mini-International Neuropsychiatric Interview (MINI) confirmed diagnosis of MDD, single or recurrent; a Hamilton Rating Scale of Depression (HRSD)-17 score of 20 or greater; at least one failed antidepressant trial in the current episode as defined by the Antidepressant Treatment History Form (ATHF); and were safe to receive TMS according to the TMS adult safety screening questionnaire.

Exclusion criteria included a lifetime MINI diagnosis of bipolar I or II, schizophrenia, schizoaffective disorder, delusional disorder, current psychotic symptoms, obsessive compulsive disorder, autism spectrum disorder; a history of epilepsy or any other major neurological disorder; a history of SCID-determined substance used disorder within the last 3 months; had concomitant major unstable medical illness; were acutely suicidal on assessment; on medications considered to be study confounds including benzodiazepines, mood stabilizers, and stimulants. Control participants were of the same age range, safe to receive TMS, and did not have any psychiatric (no history of psychiatric illness as determined by the MINI or a first degree relative with a psychiatric medical history or a second degree relative with a severe psychiatric illness) or neurological conditions.

Data were collected between July 2015 and January 2019 at the Centre for Addiction and Mental Health, Toronto, Ontario, Canada. The data came from two clinical trials (https://clinicaltrials.gov/ct2/show/NCT02472470 and https://clinicaltrials.gov/ct2/show/NCT03708172). As our goal was to investigate the cross-sectional differences between and health youth, depression and healthy controls, the baseline data collected from the two clinical trials were combined.

Experimental Design

The T1 magnetic resonance imaging (MRI) anatomical scan from each participant was used to guide TMS coil positioning during their respective TMS-EEG session. Neuro-navigation (Brainsight TMS Navigation; Rogue Resolutions) was used for targeting of cortical regions.

Participants were stimulated with 80 monophasic TMS pulses administered by a 7 cm figure-of-8 coil through two Magstim 200 stimulators (Magstim Company Ltd) at 6 sites: bilateral DLPFC, motor cortex, and IPL. Stimulation sites for the DLPFCs and IPLs were determined using MNI coordinates

(left DLPFC: −35, 45, 38; right DLPFC: 35, 45, 38; left IPL: −52, −54, 36; right IPL: 52, −51, 43). Motor cortex stimulation sites were determined by finding the optimal coil location and orientation to elicit motor-evoked potentials, as measured using electromyography, from the abductor pollicis brevis according to previously published methods and standards suggested in the field (Farzan et al. 2016). Greater detail on the resting motor threshold procedure can be found in the Supplementary Materials and Methods.

To confirm that potential findings were attributable to differences in genuine TMS probed cortical reactivity and not related to TMS-related or other artifacts, sham single pulse TMS-EEG was applied to DLPFC in a subset of participants. The sham condition consisted of the TMS coil being held perpendicular to the left or right DLPFC. The selection of the DLPFC site was randomized for each participant.

EEG Recording and Preprocessing

EEG was collected using a 64-channel Synamps 2 EEG system. Impedance for all electrodes was lowered to $\leq$ 5 kΩ. All electrodes were referenced to an electrode positioned posterior to the Cz electrode. EEG data were then recorded in DC mode with a sampling rate of 20 kHz. EEG data were preprocessed using the EEGLAB (Delorme and Makeig 2004), FieldTrip (Oostenveld et al. 2011), and TMSEEG (Atluri et al. 2016) toolboxes. Details on the preprocessing of EEG data can be found in the Supplementary Materials and Methods.

Statistical Analyses

Baseline demographics were compared between groups using independent-samples *t*-test or Chi-square test wherever appropriate.

For TMS-EEG measures of reactivity and coherence, data were compared between groups, independently for each stimulation paradigm. For TEP analysis, group comparison of TMS-EEG data was done using independent-sample *t*-statistics across all channels, from 10 to 250 ms. For coherence analysis, independent-sample *t*-statistics were used to compare coherence values between groups across the dimensions of space (i.e., channels), frequency (2–60 Hz), and time (10–500 ms). For the youth MDD group, Pearson correlations were assessed for TEPs and coherence measures with HRSD-17 and Dimensional Anhedonia Rating Scale (DARS) (Rizvi et al. 2015) scores. To investigate the potential influence of medication status on significant findings, we also compared youth MDD who were on medication at the time of testing with those who were not. To test for differences between the active and sham DLPFC stimulation conditions, dependent-sample *t*-statistics were used; the N100 was defined from 80 to 130 ms and the P200 from 150 to 250 ms. As our goal was to compare active versus sham stimulation, for each stimulation paradigm, data from healthy youth and youth MDD were combined.

All TMS-EEG analyses were corrected for multiple comparisons using cluster-based non-parametric permutation testing (Maris and Oostenveld 2007). For between group comparisons, *t*-statistics were obtained from independent-sample tests. For correlation analyses, *t*-statistics were obtained from correlation coefficients being tested as to whether they significantly differ from zero. For sham versus active comparisons, *t*-statistics were obtained from dependent-sample tests. Initial *t*-value clustering was based on an a priori threshold of $P < 0.05$. For creation of the reference distribution for the original cluster masses to be evaluated against, the data were randomized across group labels and statistical testing was carried out 2000 times in total (i.e., 2000 random permutations of the same data set) using the Monte Carlo approach. Finally, clusters in the original dataset were deemed to be significant at $P < 0.05$ (two-tailed) when compared with the reference distribution.

Logistic regression models were used to assess the ability of TMS-EEG measures to distinguish youth MDD from healthy youth. For each model, a receiver operating characteristic (ROC) curve was used to plot the sensitivity and specificity values for each measure across all potential thresholds. A greater area under the curve (AUC) for the ROC implied a better measure for classification. Logistic regression models were only assessed for neurophysiological variables that significantly differed between healthy youth and youth with depression. To obtain a single value for each participant, neurophysiological data were limited to the dimensions of the related significant cluster with the average of these values then calculated.

All statistical analyses were performed using MATLAB 2018a (Mathworks Ltd., USA) and SPSS 25.0 (SPSS Inc., USA).

Using G*Power (Faul et al. 2007, 2009), a post hoc analysis of achieved power suggested our sample size had sufficient power (>0.8) to detect primarily large effect sizes (>0.8).

Source Reconstruction

Cortical sources for all significant effects at the sensor level were reconstructed with Brainstorm (Tadel et al. 2011). Details on the source analysis can be found in the Supplementary Materials and Methods.

fMRI Data Acquisition and Analysis

Resting-state functional MRI (fMRI) data were obtained from a subset of the participants (20 of the youth MDD and all 20 healthy youth controls) and was used to confirm if the TMS-EEG targeted cortical sites belonged to their assumed functional networks. Resting state data were analyzed using the CONN toolbox (Whitfield-Gabrieli and Nieto-Castanon 2012) and SPM12, both implemented in MATLAB 2018a (Mathworks Ltd, USA). Details on the preprocessing and analysis of the fMRI data can be found in the Supplementary Materials and Methods.

Results

Demographic and Clinical Characteristics

Demographic and clinical characteristics are presented in Table 1. A total of 29 youth MDD exhibited treatment-resistant depression. Furthermore, 14 youth MDD were on medication (Table S1). The number of participants with available TMS-EEG data across the six stimulation sites were: left DLPFC (controls = 19, youth MDD = 42), right DLPFC (controls = 17, youth MDD = 41), left motor cortex (controls = 18, youth MDD = 15), right motor cortex (controls = 19, youth MDD = 16), left IPL (controls = 20, youth MDD = 37), and right IPL (controls = 19, youth MDD = 37).

Functional Connectivity of the Six Cortical Sites in Healthy Youth and Youth MDD

Resting-state functional connectivity maps suggested that each aforementioned seed was part of their assumed networks,

Table 1 Demographic and clinical data

Characteristic	Youth MDD	Healthy youth	*P*-value
Sample size, no.	45	20	NA
Age, mean (SD)	20.8 (2.64)	21.6 (1.88)	0.256
Number of males, no. (%)	18 (40)	9 (45)	0.706
Education, mean (SD)	13.2 (2.5)	15.2 (1.70)	0.002
Employment status, no. (%) employed	14 (31)	8 (40)	0.574
HRSD-17, mean (SD)	22.04 (2.40)	NA	NA
BDI-II, mean (SD)	36.13 (8.45)	NA	NA
DARS, mean (SD)	63 (27.90)	NA	NA
ATHF, mean (SD)	2.62 (1.90)	NA	NA

Abbreviations: MDD, major depressive disorder; HRSD-17, Hamilton depression rating scale; BDI, Beck depression inventory; DARS, dimensional anhedonia rating scale; ATHF, antidepressant treatment history form.

with full connectivity maps of the targeted sites illustrated in Figure S1.

TEP Differences between Healthy Youth and Youth MDD

For the right DLPFC, there was a significant positive effect ($P = 0.018$, Cohen $d = 1.08$) based on a cluster in the fronto-central electrodes (Fig. 1A) which temporally overlapped with the N100; this cluster indicated youth MDD to exhibit a greater right DLPFC N100 (i.e., a greater negativity peak) compared with controls (Fig. 1B). For the left DLPFC, two clusters were found which corresponded to the P200 (Fig. 1C): a negative cluster ($P = 0.022$, Cohen $d = 0.81$) over fronto-central electrodes and a positive cluster ($P = 0.01$, Cohen $d = 0.82$) in parietal and occipital electrodes; this cluster pattern indicated youth MDD to be associated with a greater left DLPFC P200 (i.e., a greater positivity peak) (Fig. 1D). For bilateral DLPFC, no clusters of significant difference were found for the P30, N45, or P60. For bilateral motor cortex and IPL stimulation, no clusters reached significance for any of the TEPs. Mean amplitude topoplots for youth with depression and healthy youth following each stimulation paradigm are presented in Figure S2.

TEP Differences between Active and Sham DLPFC Stimulation

In both the left (healthy youth $n = 7$, youth MDD $n = 17$) and right (healthy youth $n = 10$, youth MDD $n = 20$) DLPFC, the active stimulation resulted in significantly larger TEPs compared with sham (Fig. S3). For the N100 TEP, there were significant differences between the active and sham conditions for both the left (positive cluster $P = 0.0015$) and right (positive cluster $P < 0.001$; negative cluster $P = 0.0020$) DLPFC. Similarly, for the P200 TEP, there were significant differences between the active and sham conditions for both the left (positive cluster $P < 0.001$; negative cluster $P < 0.001$) and right (positive cluster $P < 0.001$; negative cluster $P < 0.001$) DLPFC.

Association between TEPs and Clinical Characteristics

The P200 component following both the left (positive cluster: $P = 0.018$; mean cluster $r = 0.40$) and right DLPFC (positive cluster: $P = 0.012$; mean cluster $r = 0.38$) stimulation exhibited a significant positive correlation with DARS scores (Fig. 2). No significant correlations were found between TEPs and HRSD-17 scores.

Coherence Differences between Healthy Youth and Youth MDD

Cluster-based permutations analyses revealed a significant negative cluster for coherence measure ($P < 0.001$, Cohen $d = 1.16$) following right DLPFC stimulation, indicating youth MDD to exhibit greater connectivity; specifically, the cluster was found predominantly in the theta (4–8 Hz) and alpha (8–12 Hz) frequency bands, between approximately 0 and 250 ms (Fig. 3). No coherence differences between groups were found for any of the other five cortical sites.

Association between Coherence and Clinical Characteristics

There were no significant associations between coherence and HRSD-17 or DARS scores.

Classification Accuracy

We assessed whether TMS-EEG measures that were found to be significantly different between groups could predict group assignment (healthy youths or youth MDD). Accordingly, three different logistic regression models were assessed using: right DLPFC mean coherence, right DLPFC mean N100, and left DLPFC mean P200 values (Fig. S4). All three models were found to be significant ($P < 0.001$), with the following characteristics: right DLPFC coherence model (AUC: 0.90, sensitivity: 0.83, specificity: 0.82, classification accuracy: 0.83), right DLPFC N100 model (AUC: 0.86, sensitivity: 0.82, specificity: 0.78, classification accuracy: 0.79), and left DLPFC P200 model (AUC: 0.74, sensitivity: 0.64, specificity: 0.79, classification accuracy: 0.69).

Medication Status Sub-Analysis

We investigated whether the increased right DLPFC N100, right DLPFC coherence, and left DLPFC P200 findings could be related to medications. For right DLPFC N100 and coherence, there were data from 14 medicated and 27 non-medicated participants; for left DLPFC P200, there were data from 14 medicated and 28 non-medicated participants. There were no significant differences in any of these measures between medicated and non-medicated youth MDD participants.

Source Reconstruction

TEP N100 Component

Youth MDD were found to exhibit greater activity in the following regions (threshold of $P < 0.01$; Fig. S5A): left ($t = 3.13$, Cohen $d = 0.83$) and right ($t = 2.92$, Cohen $d = 0.78$) middle anterior part of the cingulate gyrus and sulcus, right middle posterior part of the cingulate gyrus and sulcus ($t = 2.68$, Cohen $d = 0.71$), left ($t = 2.99$, Cohen $d = 0.80$) and right ($t = 2.76$, Cohen $d = 0.73$) superior frontal gyrus, left superior frontal sulcus ($t = 3.04$, Cohen $d = 0.81$), left intraparietal sulcus ($t = 2.65$, Cohen $d = 0.71$), and left ($t = 2.98$, Cohen $d = 0.80$) and right ($t = 2.85$, Cohen $d = 0.76$) pericallosal sulcus.

TEP P200 Component

Youth MDD exhibited greater activity in the (threshold of $P < 0.05$; Fig. S5B): right posterior-ventral part of the cingulate

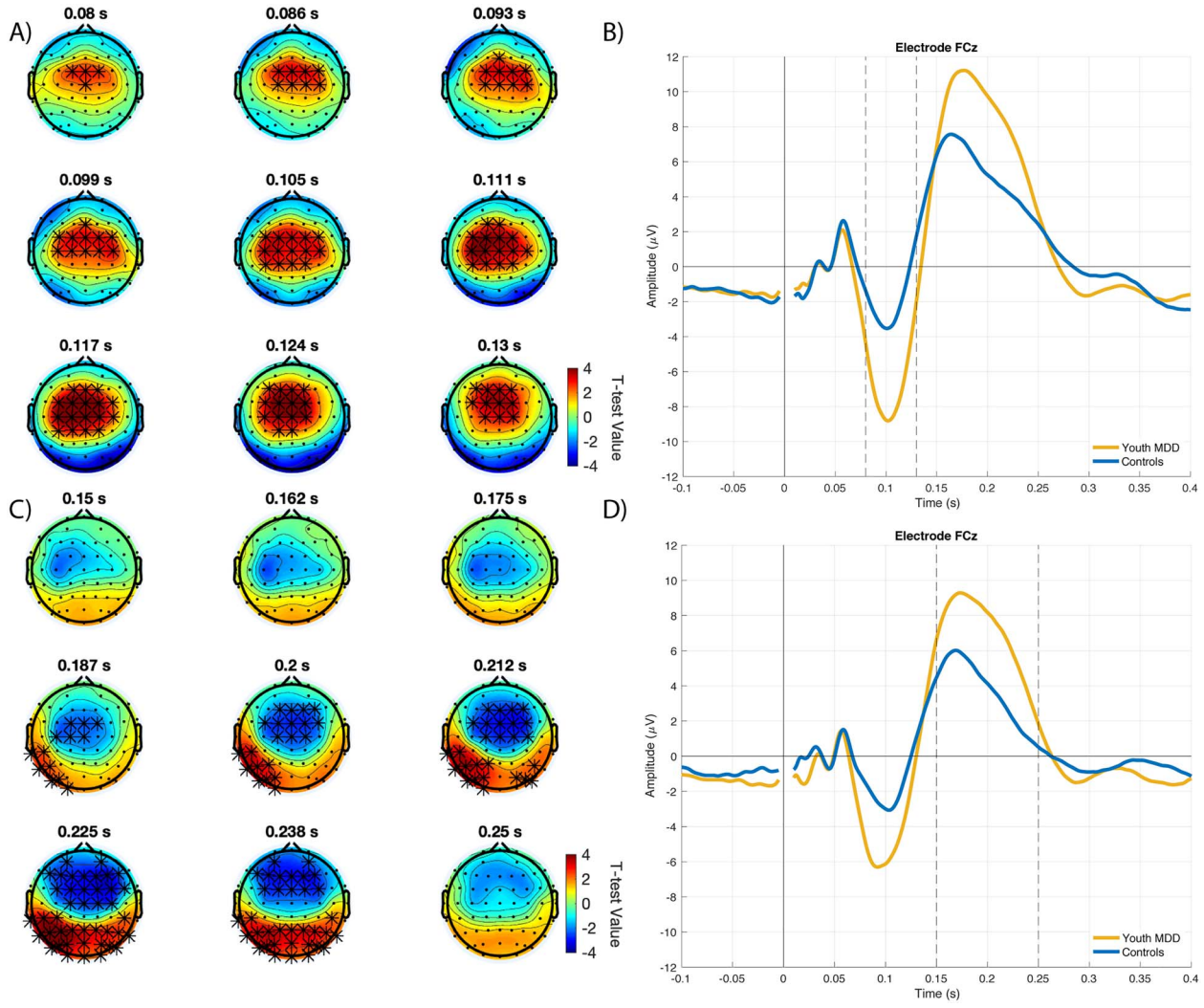

Figure 1. TEP differences following left and right DLPFC stimulation between healthy youth and youth MDD. *A*. Right DLPFC N100 differences. Topoplots illustrate all the independent-sample *t*-statistics belonging to the single cluster that was found to be significant following cluster-based correction for multiple comparisons. Electrodes illustrated with asterisks are those that belong to the significant cluster. *B*. TEP plot of electrode FCz for right DLPFC stimulation, illustrating the N100 difference between groups. *C*. Left DLPFC P200 differences. Topoplots illustrate all the independent-sample t-statistics belonging to the two clusters that were found to be significant following cluster-based correction for multiple comparisons. Electrodes illustrated with asterisks are those that belong to a significant cluster. *D*. TEP plot of electrode FCz for left DLPFC stimulation, illustrating the P200 difference between groups.

cortex ($t = 2.34$, Cohen $d = 0.62$), right central sulcus ($t = 2.16$, Cohen $d = 0.58$), right marginal branch of the cingulate sulcus ($t = 2.01$, Cohen $d = 0.54$), right lateral occipito-temporal sulcus ($t = 2.16$, Cohen $d = 0.58$), left ($t = 2.14$, Cohen $d = 0.57$) and right ($t = 2.08$, Cohen $d = 0.56$) pericallosal sulcus, and the right inferior part of the precentral sulcus ($t = 2.20$, Cohen $d = 0.59$).

TMS-EEG Connectivity

Imaginary coherence (Nolte et al. 2004) was also assessed in the source space; functional connectivity at the source level is often preferred to the sensor level as the former can be related to anatomical findings from other techniques with high spatial resolution, such as anatomical and fMRI, or animal electrophysiology (Gross et al. 2013). Here, we limited our frequency range of interest to 4–20 Hz, based on the minimum and maximum frequency values reported in the significant right DLPFC coherence cluster found at the sensor level. A region of interest approach was taken, where the coherence between the right DLPFC (defined at the same MNI coordinates as used in the TMS-EEG sessions) and all other regions defined by the Destrieux Atlas (Destrieux et al. 2010) was assessed between groups. Regions in which youth with MDD exhibited greater coherence with the right DLPFC (threshold of $P < 0.025$) are highlighted in Figure 4, and include the left rostral anterior cingulate cortex, the left angular gyrus, and the right precuneus. Mean coherence between the right DLPFC and all other regions as defined by the Destrieux Atlas for youth with depression and healthy youth are presented in Figure S6.

Discussion

To our knowledge, this is the first study to comprehensively probe and assess cortical reactivity and connectivity across several brain networks in youth MDD and compare them against age-matched healthy youths. No studies to date have assayed the neurophysiology of non-motor regions, such as DLPFC, using

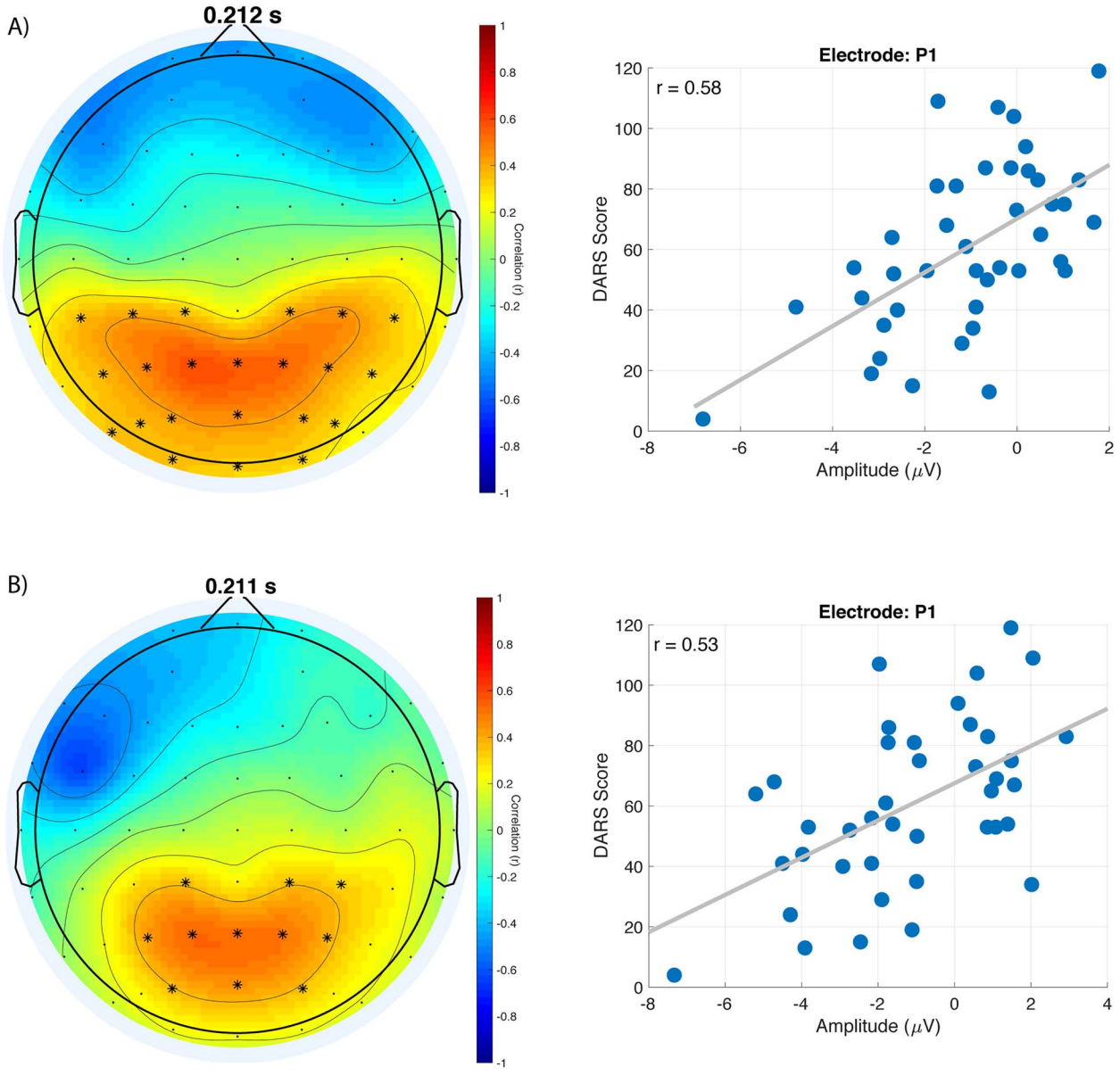

Figure 2. Correlation between left and right DLPFC P200 and DARS scores in youth MDD. Topoplots and scatter plots for A. left DLPFC and B. right DLPFC, showing the significant association between their respective P200 and DARS scores. Topoplots represent the correlation values across electrodes at the time indicated above the topoplot. Electrodes illustrated with asterisks are those that belong to the significant correlation cluster. Scatterplots show the association between DARS scores and amplitude of the electrode indicated above the scatterplot, at the time indicated above the corresponding topoplot.

TMS-EEG in youth MDD, a region critically implicated in the pathophysiology of depression (Koenigs and Grafman 2009). Our key findings imply that youth depression is associated with brain region and network-specific alterations in TMS-EEG metrics of cortical reactivity and connectivity, with links to clinical symptoms. These alterations, which included increased cortical inhibition and coherence, were specifically found following stimulation of the DLPFC and not the motor cortex or IPL. Furthermore, anhedonia was found to be correlated with the DLPFC P200; no associations were found between clinical symptoms and neurophysiological features of the motor cortex or IPL.

Both the N100 and P200 TEPs were found to be larger following stimulation of DLPFC of youth with MDD. The N100, which is suggested to reflect $GABA_B$ neurotransmission (Premoli et al. 2014), was found to be significantly greater for the right DLPFC of youth MDD. Source localization attributed this greater N100 in youth MDD to greater activity in the superior frontal gyrus as well as in the anterior cingulate cortex. This finding of a greater N100 being reported in those with depression is in partial accordance with a recent study which found adults with MDD to exhibit a greater left DLPFC N100 compared with healthy age-matched controls (Voineskos et al. 2018); the study did not assay the right DLPFC. Our findings appear in contrast with the GABA deficit hypothesis of depression, which posits that a deficit in GABAergic neurotransmission may be related to depressive symptoms (Luscher et al. 2011). Indeed,

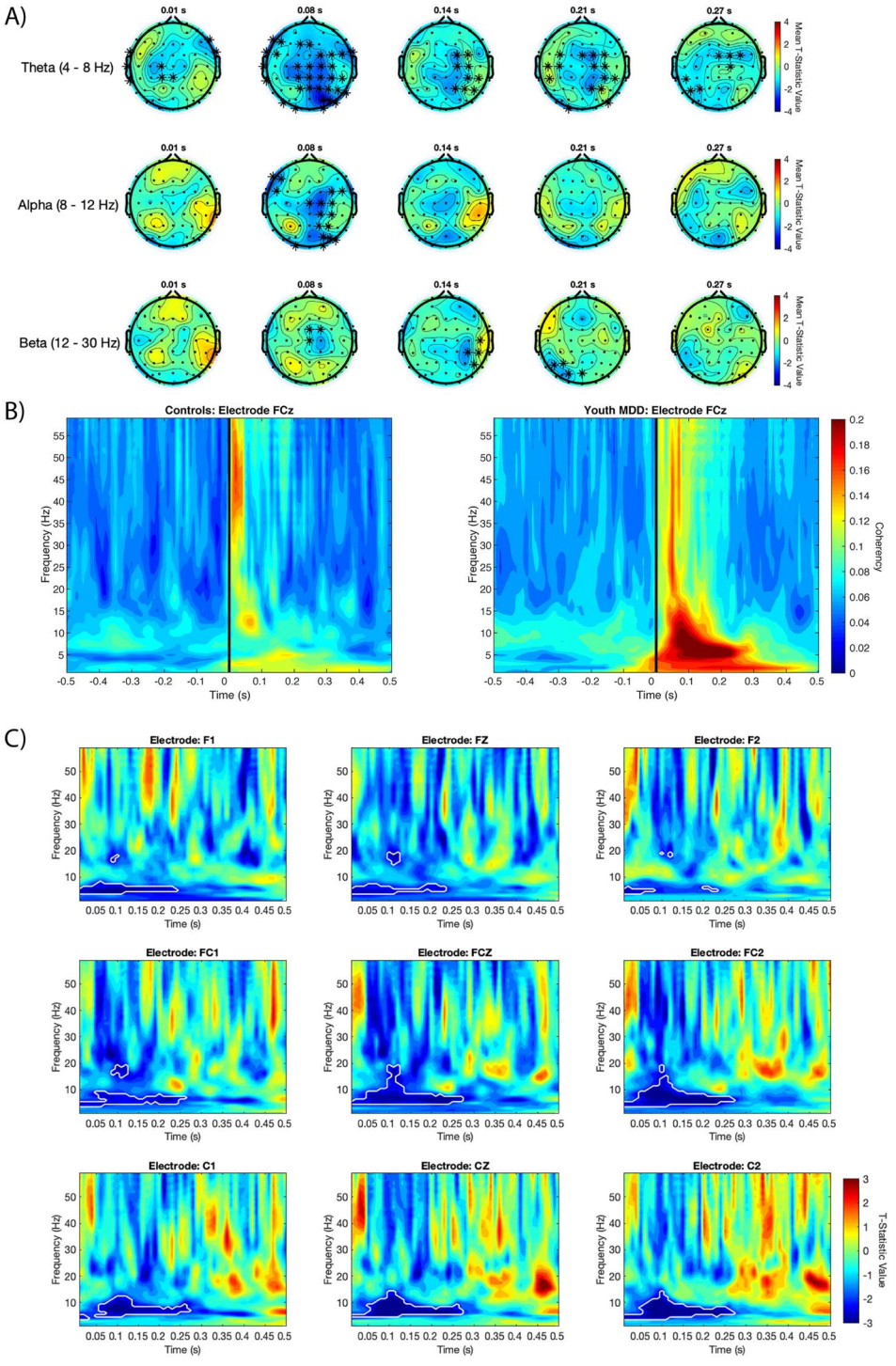

Figure 3. Right DLPFC coherence differences between healthy youth and youth MDD. *A*. Topoplots of mean *t*-statistic values for theta, alpha and beta frequency bands at times shown above each topoplot. Positive *t*-statistic values represent healthy controls exhibiting greater coherence than youth MDD, and vice-versa for negative *t*-statistic values. *T*-statistic values were averaged across each frequency band to provide visualization of where groups differed. Electrodes illustrated with an asterisk belong to the single significant negative cluster. *B*. Group average coherence values at electrode FCz for healthy controls and youth MDD. Black vertical line at time 0 represents the TMS pulse onset. *C*. Time-frequency plots of independent-sample *t*-statistics for frontocentral electrodes. Positive *t*-statistic values represent healthy controls exhibiting greater coherence than youth MDD, and vice-versa for negative *t*-statistic values. *T*-statistic values enclosed in the white border belong to the single significant negative cluster found for right DLPFC stimulation, representing the right DLPFC of youth MDD to have significantly greater coherence than healthy controls.

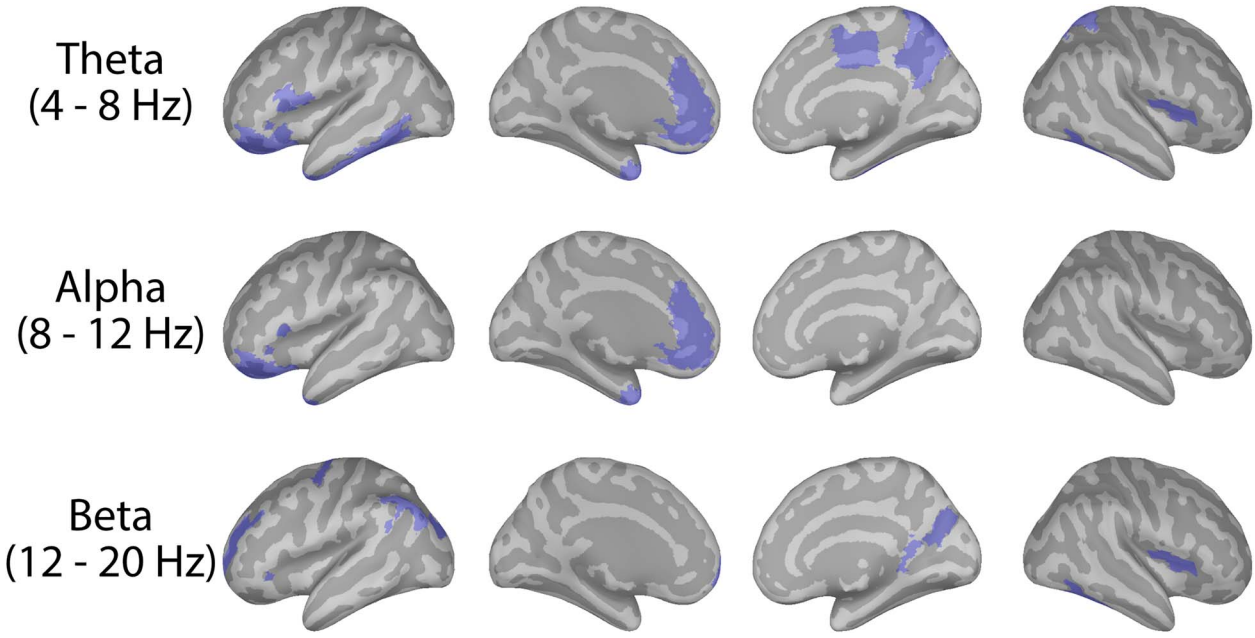

Figure 4. Group differences in functional connectivity between the right DLPFC and other cortical regions at the source level. Cortical maps illustrate which regions (in blue), as defined by the Destrieux Atlas, exhibited significantly greater coherence with the right DLPFC in youth MDD compared to healthy controls, at the uncorrected threshold of $P < 0.025$. For each participant, the imaginary coherence between each region, as defined by the Destrieux Atlas, and the right DLPFC was calculated, and then averaged within each of the frequency bands of interest (i.e., theta, alpha, and beta). Within each frequency band, independent-sample *t*-tests were then conducted to assess for which regions the coherence values significantly differed between youth with depression and healthy youth.

various markers of GABA have been reported to be diminished in adult MDD (Rajkowska et al. 2007; Levinson et al. 2010; Guilloux et al. 2012). However, it is unclear whether such markers in any part reflect inhibitory neurotransmission; rather, a decrease in GABA neuronal density or concentration may be related to an increase of GABA turnover postsynaptically, which may in turn lead to an increase of inhibitory neurotransmission (Voineskos et al. 2018). We also note that conventional antidepressants, such as selective serotonin reuptake inhibitors, have been found to increase GABA levels (Möhler 2012; Luscher and Fuchs 2015). However, our sub-analysis revealed no N100 differences between youth MDD on medication versus those not on medication at the time of testing.

In contrast, the P200 component was found to be greater following left DLPFC stimulation in youth MDD. Although the neurophysiological origin remains unknown, this component has been shown to be modulated by repetitive TMS, suggesting it to reflect in part cortical reactivity (Chung et al. 2017). Source localization suggested that the higher P200 observed following left DLPFC stimulation was linked to greater activity in the cingulate cortex in youth MDD. This may be linked to the excessive connectivity between the left DLPFC and parts of the cingulate cortex as reported in adults with depression (Ye et al. 2012). The P200 following stimulation of both the left and right DLPFC was also found to be correlated with levels of anhedonia, with lesser amplitude of the P200 being associated with greater severity of anhedonia. Anhedonia is reported by approximately 74% of youth suffering from depression (Yorbik et al. 2004), is a factor associated with an increased risk of suicidal behavior (Auerbach et al. 2015), and is a negative predictor of treatment response in youth (McMakin et al. 2012). It thus remains critical that neurobiological markers of anhedonia in this population continue to be explored; our findings suggest that the P200 component following TMS-EEG applied to DLPFC may be such a marker and may be used as a target of rTMS therapies for reducing anhedonia-related symptoms in youth MDD. Such rTMS treatments may also improve response to other classes of antidepressants, as anhedonia has been reported as being a predictor of poor response to medications (McMakin et al. 2012) and brain stimulation (Dhami et al. 2019).

MDD in general has been characterized by the dysregulation of functional networks (Kaiser et al. 2015), with youth reported to exhibit similar aberrations (Cullen et al. 2009; Zhu et al. 2012). However, a limitation of the connectivity insight offered by these aforementioned fMRI studies is that they are limited to < 1 Hz frequencies and provide no casual inference between regions. The DLPFC showed a significant difference in coherence measures between youth MDD and controls; this region has been reported to exhibit hyper-connectivity in both depressed youth (Jiao et al. 2011; Jin et al. 2011) and adults (Ye et al. 2012). The reduction of this increased DLPFC connectivity has also been implicated in the successful treatment of MDD (Perrin et al. 2012), suggesting it to have a role in the pathophysiology of MDD. Our sensor-level results in general corroborate fMRI findings, as the right DLPFC of youth MDD showed hyper-connectivity compared with controls. However, our results offer the novel TMS-EEG finding that this increased causal connectivity is potentially relayed from the DLPFC and extends predominately into the theta and alpha range. Additionally, right DLPFC connectivity, as measured by TMS-EEG, was found to exhibit very good classifying characteristics, and thus may be a biomarker worthy of further investigation.

Although speculative, a possible explanation for the observed increased right DLPFC connectivity in youth MDD may relate to it being coupled with regions of the default mode network. For instance, youth MDD exhibited greater coherence between the

right DLPFC and rostral ACC in the theta and alpha frequency. The connectivity between the DLPFC and ACC, a region commonly linked to the default mode network (Buckner et al. 2008), has been reported as being greater in youth (Davey et al. 2012) and adults (Sheline et al. 2010; Liston et al. 2014; Hadas et al. 2019) with depression. The DLPFC N100, which source analysis localized to the ACC, was also greater in youth MDD and has been linked to the DLPFC's connectivity with the subgenual cingulate cortex (Hadas et al. 2019). Finally, the right DLPFC of youth MDD exhibited greater coherence with the angular gyrus and precuneus, core nodes of the default mode network (Buckner et al. 2008; Fransson and Marrelec 2008). With regard to the increased theta and alpha band connectivity found in youth with MDD, this may reflect the dysregulation of the cognitive control-related frontoparietal network. The DLPFC is a major node of this network (Vincent et al. 2008) and is believed to be functionally connected via theta and alpha frequency band synchrony to other regions of this network (e.g., superior parietal regions) to support processes such as attention (von Stein and Sarnthein 2000; Sellers et al. 2016). Altogether, our findings suggest that the right DLPFC of youth with depression primarily exhibits elevated connectivity with regions belonging to the default mode network. This evidence provides support to the notion that depression is linked to an imbalance between large-scale functional networks (Kaiser et al. 2015). However, due to the causality provided by TMS, we are able to infer that this heightened connectivity between the DLPFC and parts of the default mode network potentially stems from the DLPFC and not other brain regions; this was further corroborated by no connectivity differences being reported from stimulation of the default mode network-related bilateral IPLs.

In the context of treatment, attenuating this elevated DLPFC connectivity to other regions, such as the ACC, through brain stimulation has been shown to have clinical efficacy (Perrin et al. 2012; Liston et al. 2014; Hadas et al. 2019). By demonstrating a similar network dysfunction in youth MDD that is mediated by the right DLPFC, brain stimulation to this region may be a potential neurobiologically supported alternative treatment for youth with depression who have failed to respond to conventional therapies.

Limitations to our study include that no treatment naïve youth MDD patients were included, rendering it unclear as to whether our findings are generalizable to the entire youth MDD population. However, the majority of patients were unmedicated, and we identified no significant impact of medications on the reported neuromarkers, reducing the likelihood that medications may have influenced the reported results; we do note that this sub-analysis may however been underpowered due to a small sample size. There was also a sample size discrepancy between the two groups, with only 20 healthy youth being recruited versus the 45 youth with MDD.

Finally, we note another potential limitation, which is the possible contamination of the N100 and P200 components by TMS-induced somatosensory and auditory artifacts (Conde et al. 2019). However, our study uniquely incorporated several methodological and study design strategies to significantly reduce the likelihood of such contamination. First, various recommendations have been made to reduce these confounding artifacts, including the use of earplugs and a thin layer of foam on the TMS coil (ter Braack et al. 2015), both of which were used in this study. Second, we employed a cross-sectional design, in which all the participants underwent the same testing paradigm. With this design any potential artifacts would be negated in the cross-sectional comparison. Third, the study design included multiple stimulation sites. Let us assume that the N100 and P200 are, for example, auditory-related artifacts, and that youth with depression and healthy youth differ in auditory processing of the TMS click sound. If this was the case, one would expect differences in the N100 and P200 between groups to be found across all six stimulation sites, as they were all accompanied by the TMS click sound. However, we only found differences in the DLPFC, and not in the motor cortex or IPL. Thus, our regional-specific results, which were only afforded by the stimulation of multiple sites, ultimately suggests that our findings were not influenced by artifacts, but rather reflect differences in genuine cortical reactivity. Finally, our study design also included a TMS sham condition that further illustrated the significant difference in N100 and P200 component between the active and sham condition. Collectively, the observed N100 and P200 differences between youth with depression and healthy youth are very unlikely to be artifactual. However, we note that as stimulation of the DLPFC with TMS can activate frontalis muscles, which is not to be expected with stimulation of the motor cortex or IPL, this somatosensory-related component of the DLPFC TEPs remained a potential confound that could not be addressed by the current study design. Future studies which involve DLPFC stimulation may wish to incorporate a sham with a somatosensory component, such as electrical stimulation, to account for stimulation of the frontalis muscles.

Ultimately, our study found youth MDD to be associated with DLPFC dysfunction in the form of greater reactivity and altered connectivity; no differences were found when motor cortices or IPL were stimulated, suggesting this cortical dysregulation to be specific and originated by the prefrontal cortex. These markers of cortico-frontal dysfunction could serve as a biomarker to support the clinical diagnosis of youth MDD. Furthermore, these findings provide novel insight into the pathophysiology of youth MDD which may guide future novel treatments, such as non-invasive brain stimulation, which are capable of selectively modulating fronto-cortical neurophysiology.

Supplementary Material

Supplementary material can be found at *Cerebral Cortex* online.

Funding

National Institutes of Health (R01 MH113700 to P.E.C.); Mayo Clinic Foundation; and Brain and Behavior Research Foundation; Michael Smith Foundation for Health Research; and Canadian Institute of Health Research.

Notes

Prabhjot Dhami was supported by the doctoral award from Canadian Institute for Health Research (CIHR). Paul E. Croarkin has received research support from Pfizer (investigator-initiated study), Assurex (grant in kind for genotyping and supplies for investigator-initiated study), and Neuronetics, Inc. (equipment support). He served as the overall PI for a multicenter trial funded by Neuronetics and site PI for a trial funded by NeoSync, Inc. He serves as an advisor to Procter and Gamble. Daniel M. Blumberger has received research support from the CIHR, NIH, Brain Canada and the Temerty Family through the CAMH Foundation and the Campbell Research Institute. He has also received research support and in-kind equipment support for

an investigator-initiated study from Brainsway Ltd, and he is the principal site investigator for three sponsor-initiated studies for Brainsway Ltd He received in-kind equipment support from Magventure for investigator-initiated research. He received medication supplies for an investigator-initiated trial from Indivior. He has participated in an advisory board for Janssen. Zafiris J. Daskalakis's work was supported by the Ontario Mental Health Foundation (OMHF), the Canadian Institutes of Health Research (CIHR), the National Institutes of Mental Health (NIMH) and the Temerty Family and Grant Family and through the Centre for Addiction and Mental Health (CAMH) Foundation and the Campbell Institute. In the last 5 years, Zafiris J. Daskalakis has received research and equipment in-kind support for an investigator-initiated study through Brainsway Inc and Magventure Inc. Faranak Farzan was supported by Slaight Family Centre for Youth in Transition (research funding awarded to Dr. Farzan), and Michael Smith Foundation for Health Research Scholar Award, CIHR, and the National Sciences and Engineering Research Council. Sravya Atluri, Jonathan C. Lee and Yuliya Knyahnytska have nothing to disclose. *Conflict of Interest*: None declared.

References

Atluri S, Frehlich M, Mei Y, Garcia Dominguez L, Rogasch NC, Wong W, Daskalakis ZJ, Farzan F. 2016. TMSEEG: a MATLAB-based graphical user Interface for processing electrophysiological signals during transcranial magnetic stimulation. *Front Neural Circuits*. 10:78.

Auerbach RP, Millner AJ, Stewart JG, Esposito EC. 2015. Identifying differences between depressed adolescent suicide ideators and attempters. *J Affect Disord*. 186:127–133.

Blakemore S-J, Choudhury S. 2006. Development of the adolescent brain: implications for executive function and social cognition. *J Child Psychol Psychiatry*. 47:296–312.

Bortoletto M, Veniero D, Thut G, Miniussi C. 2015. The contribution of TMS-EEG coregistration in the exploration of the human cortical connectome. *Neurosci Biobehav Rev*. 49:114–124.

Buckner RL, Andrews-Hanna JR, Schacter DL. 2008. The brain's default network. *Ann N Y Acad Sci*. 1124:1–38.

Chung SW, Lewis BP, Rogasch NC, Saeki T, Thomson RH, Hoy KE, Bailey NW, Fitzgerald PB. 2017. Demonstration of short-term plasticity in the dorsolateral prefrontal cortex with theta burst stimulation: a TMS-EEG study. *Clin Neurophysiol*. 128:1117–1126.

Conde V, Tomasevic L, Akopian I, Stanek K, Saturnino GB, Thielscher A, Bergmann TO, Siebner HR. 2019. The non-transcranial TMS-evoked potential is an inherent source of ambiguity in TMS-EEG studies. *NeuroImage*. 185:300–312.

Croarkin PE, Nakonezny PA, Lewis CP, Zaccariello MJ, Huxsahl JE, Husain MM, Kennard BD, Emslie GJ, Daskalakis ZJ. 2014. Developmental aspects of cortical excitability and inhibition in depressed and healthy youth: an exploratory study. *Front Hum Neurosci*. 8:1–9.

Cullen KR, Gee DG, Klimes-Dougan B, Gabbay V, Hulvershorn L, Mueller BA, Camchong J, Bell CJ, Houri A, Kumra S *et al*. 2009. A preliminary study of functional connectivity in comorbid adolescent depression. *Neurosci Lett*. 460:227–231.

Damoiseaux JS, Rombouts SARB, Barkhof F, Scheltens P, Stam CJ, Smith SM, Beckmann CF. 2006. Consistent resting-state networks across healthy subjects. *Proc Natl Acad Sci U S A*. 103:13848–13853.

Darmani G, Ziemann U. 2019. Pharmacophysiology of TMS-evoked EEG potentials: a mini-review. *Brain Stimul*. 12:829–831.

Davey CG, Yücel M, Allen NB, Harrison BJ. 2012. Task-related deactivation and functional connectivity of the subgenual cingulate cortex in major depressive disorder. *Front Psych*. 3:14.

Delorme A, Makeig S. 2004. EEGLAB: an open source toolbox for analysis of single-trial EEG dynamics including independent component analysis. *J Neurosci Methods*. 134:9–21.

Destrieux C, Fischl B, Dale A, Halgren E. 2010. Automatic parcellation of human cortical gyri and sulci using standard anatomical nomenclature. *NeuroImage*. 53:1–15.

Dhami P, Knyahnytska Y, Atluri S, Lee J, Courtney DB, Croarkin PE, Blumberger DM, Daskalakis ZJ, Farzan F. 2019. Feasibility and clinical effects of theta burst stimulation in youth with major depressive disorders: an open-label trial. *J Affect Disord*.

Farzan F, Vernet M, Shafi MMD, Rotenberg A, Daskalakis ZJ, Pascual-Leone A. 2016. Characterizing and modulating brain circuitry through transcranial magnetic stimulation combined with electroencephalography. *Front Neural Circuits*. 10.

Faul F, Erdfelder E, Buchner A, Lang A-G. 2009. Statistical power analyses using G*power 3.1: tests for correlation and regression analyses. *Behav Res Methods*. 41:1149–1160.

Faul F, Erdfelder E, Lang A-G, Buchner A. 2007. G*power 3: a flexible statistical power analysis program for the social, behavioral, and biomedical sciences. *Behav Res Methods*. 39: 175–191.

Fransson P, Marrelec G. 2008. The precuneus/posterior cingulate cortex plays a pivotal role in the default mode network: evidence from a partial correlation network analysis. *NeuroImage*. 42:1178–1184.

Fung SJ, Webster MJ, Sivagnanasundaram S, Duncan C, Elashoff M, Weickert CS. 2010. Expression of interneuron markers in the dorsolateral prefrontal cortex of the developing human and in schizophrenia. *Am J Psychiatry*. 167:1479–1488.

Gibbons RD, Brown CH, Hur K, Davis JM, Mann JJ. 2012. Suicidal thoughts and behavior with antidepressant treatment. *Arch Gen Psychiatry*. 69:580.

Giedd JN, Keshavan M, Paus T. 2008. Why do many psychiatric disroders emerge during adolescence? *Nat Rev Neurosci*. 9:947–957.

Gogtay N, Giedd JN, Lusk L, Hayashi KM, Greenstein D, Vaituzis AC, Nugent TF, Herman DH, Clasen LS, Toga AW *et al*. 2004. Dynamic mapping of human cortical development during childhood through early adulthood. *Proc Natl Acad Sci U S A*. 101:8174–8179.

Gross J, Baillet S, Barnes GR, Henson RN, Hillebrand A, Jensen O, Jerbi K, Litvak V, Maess B, Oostenveld R *et al*. 2013. Good practice for conducting and reporting MEG research. *NeuroImage*. 65:349–363.

Guilloux J-P, Douillard-Guilloux G, Kota R, Wang X, Gardier AM, Martinowich K, Tseng GC, Lewis DA, Sibille E. 2012. Molecular evidence for BDNF- and GABA-related dysfunctions in the amygdala of female subjects with major depression. *Mol Psychiatry*. 17:1130–1142.

Hadas I, Sun Y, Lioumis P, Zomorrodi R, Jones B, Voineskos D, Downar J, Fitzgerald PB, Blumberger DM, Daskalakis ZJ. 2019. Association of Repetitive Transcranial Magnetic Stimulation Treatment with subgenual cingulate hyperactivity in patients with major depressive disorder. *JAMA Netw Open*. 2:e195578.

Jiao Q, Ding J, Lu G, Su L, Zhang Z, Wang Z, Zhong Y, Li K, Ding M, Liu Y. 2011. Increased activity imbalance in fronto-subcortical circuits in adolescents with major depression. *PLoS One*. 6:e25159.

Jin C, Gao C, Chen C, Ma S, Netra R, Wang Y, Zhang M, Li D. 2011. A preliminary study of the dysregulation of the resting networks in first-episode medication-naive adolescent depression. *Neurosci Lett*. 503:105–109.

Kaiser RH, Andrews-Hanna JR, Wager TD, Pizzagalli DA. 2015. Large-scale network dysfunction in major depressive disorder: a meta-analysis of resting-state functional connectivity. *JAMA Psychiat*. 72:603–611.

Koenigs M, Grafman J. 2009. The functional neuroanatomy of depression: distinct roles for ventromedial and dorsolateral prefrontal cortex. *Behav Brain Res*. 201:239–243.

Leuchter AF, Cook IA, Hunter AM, Cai C, Horvath S. 2012. Resting-state quantitative electroencephalography reveals increased neurophysiologic connectivity in depression. *PLoS One*. 7:e32508.

Levinson AJ, Fitzgerald PB, Favalli G, Blumberger DM, Daigle M, Daskalakis ZJ. 2010. Evidence of cortical inhibitory deficits in major depressive disorder. *Biol Psychiatry*. 67:458–464.

Liston C, Chen AC, Zebley BD, Drysdale AT, Gordon R, Leuchter B, Voss HU, Casey BJ, Etkin A, Dubin MJ. 2014. Default mode network mechanisms of transcranial magnetic stimulation in depression. *Biol Psychiatry*. 76:517–526.

Luscher B, Fuchs T. 2015. GABAergic control of depression-related brain states. *Adv Pharmacol*. 73:97–144.

Luscher B, Shen Q, Sahir N. 2011. The GABAergic deficit hypothesis of major depressive disorder. *Mol Psychiatry*. 16:383–406.

March JS, Silva S, Petrycki S, Curry J, Wells K, Fairbank J, Burns B, Domino M, McNulty S, Vitiello B *et al*. 2007. The treatment for adolescents with depression study (TADS): long-term effectiveness and safety outcomes. *Arch Gen Psychiatry*. 64:1132–1143.

Maris E, Oostenveld R. 2007. Nonparametric statistical testing of EEG- and MEG-data. *J Neurosci Methods*. 164:177–190.

McMakin DL, Olino TM, Porta G, Dietz LJ, Emslie G, Clarke G, Wagner KD, Asarnow JR, Ryan ND, Birmaher B *et al*. 2012. Anhedonia predicts poorer recovery among youth with selective serotonin reuptake inhibitor treatment-resistant depression. *J Am Acad Child Adolesc Psychiatry*. 51:404–411.

Miller CH, Hamilton JP, Sacchet MD, Gotlib IH. 2015. Meta-analysis of functional neuroimaging of major depressive disorder in youth. *JAMA Psychiat*. 72:1045–1053.

Möhler H. 2012. The GABA system in anxiety and depression and its therapeutic potential. *Neuropharmacology*. 62:42–53.

Nolte G, Bai O, Wheaton L, Mari Z, Vorbach S, Hallett M. 2004. Identifying true brain interaction from EEG data using the imaginary part of coherency. *Clin Neurophysiol*. 115: 2292–2307.

Oostenveld R, Fries P, Maris E, Schoffelen J-M. 2011. FieldTrip: open source software for advanced analysis of MEG, EEG, and invasive electrophysiological data. *Comput Intell Neurosci*. 2011:156869.

Perrin JS, Merz S, Bennett DM, Currie J, Steele DJ, Reid IC, Schwarzbauer C. 2012. Electroconvulsive therapy reduces frontal cortical connectivity in severe depressive disorder. *Proc Natl Acad Sci U S A*. 109:5464–5468.

Premoli I, Castellanos N, Rivolta D, Belardinelli P, Bajo R, Zipser C, Espenhahn S, Heidegger T, Muller-Dahlhaus F, Ziemann U. 2014. TMS-EEG signatures of GABAergic neurotransmission in the human cortex. *J Neurosci*. 34:5603–5612.

Rajkowska G, O'Dwyer G, Teleki Z, Stockmeier CA, Miguel-Hidalgo JJ. 2007. GABAergic neurons immunoreactive for calcium binding proteins are reduced in the prefrontal cortex in major depression. *Neuropsychopharmacology*. 32:471–482.

Rizvi SJ, Quilty LC, Sproule BA, Cyriac A, Michael Bagby R, Kennedy SH. 2015. Development and validation of the dimensional anhedonia rating scale (DARS) in a community sample and individuals with major depression. *Psychiatry Res*. 229:109–119.

Sellers KK, Yu C, Zhou ZC, Stitt I, Li Y, Radtke-Schuller S, Alagapan S, Fröhlich F. 2016. Oscillatory dynamics in the frontoparietal attention network during sustained attention in the ferret. *Cell Rep*. 16:2864–2874.

Sheline YI, Price JL, Yan Z, Mintun MA. 2010. Resting-state functional MRI in depression unmasks increased connectivity between networks via the dorsal nexus. *Proc Natl Acad Sci U S A*. 107:11020–11025.

Tadel F, Baillet S, Mosher JC, Pantazis D, Leahy RM. 2011. Brainstorm: a user-friendly application for MEG/EEG analysis. *Comput Intell Neurosci*. 2011:1–13.

ter Braack EM, de Vos CC, van Putten MJAM. 2015. Masking the auditory evoked potential in TMS–EEG: a comparison of various methods. *Brain Topogr*. 28:520–528.

van den Heuvel MP, Hulshoff Pol HE. 2010. Exploring the brain network: a review on resting-state fMRI functional connectivity. *Eur Neuropsychopharmacol*. 20:519–534.

Vincent JL, Kahn I, Snyder AZ, Raichle ME, Buckner RL. 2008. Evidence for a frontoparietal control system revealed by intrinsic functional connectivity. *J Neurophysiol*. 100: 3328–3342.

Voineskos D, Blumberger DM, Zomorrodi R, Rogasch NC, Farzan F, Foussias G, Rajji TK, Daskalakis ZJ. 2018. Altered transcranial magnetic stimulation-electroencephalographic markers of inhibition and excitation in the dorsolateral prefrontal cortex in major depressive disorder. *Biol Psychiatry*. 85:477–486.

von Stein A, Sarnthein J. 2000. Different frequencies for different scales of cortical integration: from local gamma to long range alpha/theta synchronization. *Int J Psychophysiol*. 38: 301–313.

Whitfield-Gabrieli S, Nieto-Castanon A. 2012. *Conn*: a functional connectivity toolbox for correlated and anticorrelated brain networks. *Brain Connect*. 2:125–141.

Ye T, Peng J, Nie B, Gao J, Liu J, Li Y, Wang G, Ma X, Li K, Shan B. 2012. Altered functional connectivity of the dorsolateral prefrontal cortex in first-episode patients with major depressive disorder. *Eur J Radiol*. 81:4035–4040.

Yorbik O, Birmaher B, Axelson D, Williamson DE, Ryan ND. 2004. Clinical characteristics of depressive symptoms in children and adolescents with major depressive disorder. *J Clin Psychiatry*. 65:1654–1659 quiz 1760–1761.

Zalsman G, Oquendo MA, Greenhill L, Goldberg PH, Kamali M, Martin A, Mann JJ. 2006. Neurobiology of depression in children and adolescents. *Child Adolesc Psychiatr Clin N Am*. 15:843–868, vii–viii.

Zhu X, Wang X, Xiao J, Liao J, Zhong M, Wang W, Yao S. 2012. Evidence of a dissociation pattern in resting-state default mode network connectivity in first-episode, treatment-naive major depression patients. *Biol Psychiatry*. 71:611–617.